Environmental Science and Pollution Research (2018) 25:29493–29504
https://doi.org/10.1007/s11356-018-2942-x

RESEARCH ARTICLE

Photocatalytic degradation of azo dye using core@shell nano-TiO_2 particles to reduce toxicity

Nesrin Ozmen[1] · Sema Erdemoglu[2] · Abbas Gungordu[3] · Meltem Asilturk[4] · Duygu Ozhan Turhan[3] · Emrah Akgeyik[2] · Stacey L. Harper[5] · Murat Ozmen[3]

Received: 9 April 2018 / Accepted: 8 August 2018 / Published online: 22 August 2018

Abstract

Clean and safe water is fundamental for human and environmental health. Traditional remediation of textile dye-polluted water with chemical, physical, and biological processes has many disadvantages. Due to this, nano-engineered materials are drawing more attention to this area. However, the widespread use of nano-particles for this purpose may lead to photocatalytic degradation of xenobiotics, while increasing the risk of nano-particle-induced ecotoxicity. Therefore, we comparatively evaluated the toxicity of novel synthesized core@shell TiO_2 and SiO_2 nano-particles to embryonic stages of *Danio rerio* and *Xenopus laevis*. The ability of photocatalytic destruction of the synthesized nano-particles was tested using toxic azo dye, disperse red 65, and the effects of reducing the toxicity were evaluated. The reflux process was used to synthesize catalysts in the study. The samples were characterized by scanning electron microscopy, X-ray fluorescence spectroscopy, X-ray diffractometry, BET surface area, and UV–vis-diffuse reflectance spectra. It was determined that the synthesized nano-particles had no significant toxic effect on *D. rerio* and *X. laevis* embryos. On the other hand, photocatalytic degradation of the dye significantly reduced lethal effects on embryonic stages of the organisms. Therefore, we suggest that specific nano-particles may be useful for water remediation to prevent human health and environmental impact. However, further risk assessment should be conducted for the ecotoxicological risks of nano-particles spilled in aquatic environments and the relationship of photocatalytic interaction with nano-particles and xenobiotics.

Keywords Core/shell nano-TiO_2 · Azo dye · Toxicity · Photodegradation · *Danio rerio* · *Xenopus laevis*

Introduction

Water pollution, providing safe water sources, and eco-friendly water treatment for human and environmental health are important problems around the world. Some methods involving biological and physical chemical processes are not sufficient for the purification of various industrial pollutants in water resources (Sonune and Ghate 2004). Therefore, alternative photocatalytic water treatment techniques and nano-particles (NPs) with high photocatalytic properties may be useful for this purpose in order to remove contaminants from the polluted water (Ni et al. 2007). Titanium dioxide (TiO_2) is one specific option already in commerce with over 165×10^6 metric tons of titanium in bulk and nano-forms being produced worldwide in the last decade (Gupta and Tripathi 2011; Jovanovic 2015). TiO_2 NPs are also widely used in photocatalysis, self-cleaning coatings, antibacterial coatings on medical devices, and many other applications because of their photocatalytic activity, benefit-to-cost ratio, as well as good chemical stability (Chatterjee et al. 2014; Clemente et al. 2014). Wastewater treatment with TiO_2 NPs has markedly increased in recent years due to their ability to remediate organic pollutants, which is enhanced by their high relative surface area in aqueous environments (Hariharan 2006;

Responsible editor: Philippe Garrigues

✉ Murat Ozmen
murat.ozmen@inonu.edu.tr

[1] Department of Mathematics and Science Education, Faculty of Education, Inonu University, 44280 Malatya, Turkey

[2] Department of Chemistry, Faculty of Arts and Science, Inonu University, 44280 Malatya, Turkey

[3] Laboratory of Environmental Toxicology, Department of Biology, Faculty of Arts and Science, Inonu University, 44280 Malatya, Turkey

[4] Department of Materials Science and Engineering, Faculty of Engineering, Akdeniz University, 07058 Antalya, Turkey

[5] Department of Environmental and Molecular Toxicology, Oregon State University, Corvallis, OR 97331, USA

Ijadpanah-Saravi et al. 2016; Nogueira et al. 2015; Robert et al. 2017; Shanmugam et al. 2006; Yang et al. 2012). Applications of TiO_2 for photocatalysis depends on physical properties such as morphology and particle size (Zhang et al. 2008). However, NP agglomeration, phase transformation, reduction in surface area after thermal processing, and lack of visible light photoactivity due to broad band void are some problems with nano-scale TiO_2 (Habibi and Bagheri 2017; Hu et al. 2003; Pan et al. 2012). To overcome most of the problems with TiO_2 NPs, titania can be coated to form a layer on the surface of thermally stable, low cost, and high surface area core materials such as SiO_2, ZrO_2, and Fe_2O_3. For this reason, core@shell (CS) structures have attracted more attention in recent years because they provide better physical chemical properties and more secure nano-materials than individual components (Burello 2015; Lee et al. 2007). Titania powders with large surface areas are not thermally stable and can easily lose surface areas at high temperatures. Therefore, researchers in recent years have been investigating titania coating on silica core and vice versa (Caruso et al. 2001; Demirors et al. 2009; Fujiwara et al. 2017; Khan and Jensen 2007; Shiba et al. 2016). Silica is one of the best core materials for preparing CS structures because their surface chemistry is well understood; they have high adsorption capacity and their optical transparency in the wavelength region is where TiO_2 absorbs (Ullah et al. 2015).

Additional concerns arise when producing NPs on a large scale because some NPs can be toxic to living systems due to their ability to penetrate bio-membranes and interfere with basal metabolic reactions within cells. Because of their size, NPs can easily translocate throughout the body by the circulatory system and breach neural networks (Gramowski et al. 2010). NPs can cause a variety of developmental anomalies in the organism, especially in the aquatic environment (Garcia-Alonso et al. 2014; Ostaszewska et al. 2016). In addition to their potential for uptake and toxicity, some NPs can also accumulate in the body when the body does not have any mechanism to eliminate them from the system or process metabolically (Chatterjee et al. 2014). In addition, NPs can accumulate in aquatic environments, increasing ecological risk concerns. According to their surface properties and nano-size, they may bind and transport toxic chemical pollutants, cause toxic metabolites, and generate reactive radicals (Faria et al. 2014; Moore 2006). NPs entering water systems may also cause environmental problems because of their high tendency to interact with toxic pollutants in the water ecosystem. Most TiO_2 NPs are discharged to sewage but recovery of TiO_2 NPs from water treatment plants is very difficult. Like other types of NPs, increasing use of TiO_2 NPs has raised significant concerns about their toxicity to aquatic organisms but we still have limited information on their ecotoxic effects and interactions with other environmental pollutants. It is estimated that the environmental concentrations of nano-TiO_2 in surface water may be in the range of 0.7–16 mg L^{-1} depending on the intensity of their use (Mueller and Nowack 2008). However, effluent concentrations may range from 181 to 1233 mg L^{-1} (Westerhoff et al. 2011).

In this work, the toxicity of pure novel synthesized TiO_2, SiO_2 and core@shell NPs, toxicity of azo dye (disperse red 65; DR65), and photodegradation capacity of the NPs on azo dye have been investigated. The other objective of this study was to comparatively evaluate ecotoxicological potentials using the embryonic zebrafish and *Xenopus laevis* tadpoles. These organisms were selected as models that represent relatively different trophic levels and important components of aquatic ecosystems.

Materials and methods

Chemicals and reagents

Titanium-*iso*-propoxide [Ti $(OPri)_4$, TTIP, 97%) and tetraethyl orthosilicate [Si $(OEt)_4$, TEOS, 99%) purchased from ABCR was used as titanium or silica sources for the preparation of photocatalysts. All other chemicals and reagents used for NP synthesis were purchased from Merck (Germany) or Sigma-Aldrich (USA). Deionized water was used for the hydrolysis of TTIP with TEOS and for the preparation of all sols and solutions. To investigate the photocatalytic activity of the synthesized NPs on the azo dye, disperse red 65 (DR65) (C.I. 11228; $C_{18}H_{18}C_lN_5O_2$) (BDH Chemical Ltd., Poole, UK) stock solution was prepared in purified water.

Synthesis of CSNPs

The reflux process was chosen to synthesize all catalysts except for the SiO_2 synthesis. Pure TiO_2 NP was synthesized as being the core material in which Ti $(OPri)_4$ was used as the starting material. Ten grams of Ti $(OPri)_4$ was dissolved in a glass flask containing 30 ml of *n*-propanol. After stirring for a few minutes at room temperature, the alkoxide solution was drop wise added to the solution, which consists of *n*-propanol, HCl, and H_2O. The ratios for *n*-PrOH/Ti $(OPri)_4$, HCl/Ti $(OPri)_4$, and H_2O/Ti $(OPri)_4$ in this solution are 100, 0.2, and 50 mol/mol, respectively. The last mixture was stirred at 130 °C in reflux for 6 h. Then, the mixture was cooled down to room temperature. After separating obtained solids through centrifugation (Hettich Zentrifugen Universal 320), nano-TiO_2 powder was washed with absolute ethanol and then dried in a vacuum sterilizer (Binder VD23) at 50 °C for 24 h. For the preparation of pure SiO_2 NPs, 10 g of Si $(OEt)_4$ was dissolved in absolute ethanol. After stirring for a few minutes at room temperature, the NH_3 solution was drop wise added to the sol-solution in which EtOH/Si $(OEt)_4$ and NH_3/Si $(OEt)_4$ ratios (*n*/*n*) were 0.0119 and 0.319, respectively. The reaction was

allowed to continue for 6 h at 60 °C. The obtained nano-powder was separated by centrifugation and washed with de-ionized water several times before being dried in a vacuum sterilizer at 60 °C for 24 h. To prepare TiO_2 core and SiO_2 shell (TiO_2@SiO_2), 1 g of TiO_2 NPs was dispersed in 20 ml of ethanol-water using a sonicator. It was transferred to a two-necked glass flask and diluted with 80 ml of ethanol. Then, 2 g of the Si $(OEt)_4$ and 6 ml of NH_3 were drop wise added to the above sol-solution. The final solution was stirred until a homogeneous solution was obtained (~ 4 h at room temperature). The powder was separated through centrifuging and washed with absolute ethanol at pH = 7 and dried in a vacuum sterilizer at 60 °C for 24 h. To obtain both consisting of SiO_2 core, 13 g of Si $(OEt)_4$ was dissolved in a two-necked glass flask containing 270 ml of ethanol before the NH_3 solution was drop wise added to this sol-solution for preparing SiO_2@TiO_2 structure. EtOH/Si $(OEt)_4$, NH_3/Si $(OEt)_4$, and H_2O/Si $(OEt)_4$ ratios (*n*/*n*) were 0.0104, 4.175, and 11.0 mol/mol, respectively, in this solution. After stirring for 6 h at 50 °C in reflux, 16 g of Ti $(OPri)_4$ was drop wise added to the sol-solution. The reaction was allowed to continue for 8 h at room temperature in reflux. The synthesized powder was separated through centrifugation and washed with absolute ethanol before being dried in a vacuum sterilizer. Finally, we proceeded to calcination, followed by annealing at 500 °C for 3 h.

Nano-particle characterization

The surface morphologies of the catalysts were observed using a scanning electron microscope (SEM; Leo Evo 40 model, Carl Zeiss) at Inönü University in Malatya, Turkey, and a field emission scanning electron microscope (FE-SEM; Ultra 55 model, Carl Zeiss) at the Center for Advanced Materials Characterization, University of Oregon (Eugene, OR). The crystalline structures of synthesized CS and pure NPs were determined by x-ray diffraction (XRD; Giegerflex D/Max B, Rigaku) using Cu Kα radiation in the range 2θ:10–80°. The crystallite size of the NPs was calculated from XRD peak of (101) spacing according to the Scherrer equation and the structures of the CSNPs were observed by transmission electron microscope (TEM; Titan 80-200 model, FEI) at the Linus Pauling Institute, Oregon State University (Corvallis, OR). FTIR spectra for the samples were obtained using a system Perkin Elmer Precisely Spectrum One in the range 4000–350 cm^{-1}. Zeta potential and particle size distribution of the synthesized catalysts were measured by dynamic light scattering (DLS; Zetasizer Nano-ZS model, Malvern Ins. Ltd.). Specific surface areas (S_{BET}) of the particles were measured using a BET (Brunauer-Emmett-Teller) analyzer (Micromeritics Tristar 3030 model). BET surface areas were measured by N_2 adsorption/desorption at 77 K. The specific surface areas were calculated from BET-measured nitrogen adsorption isotherms and the pore size distributions were calculated using density functional theory (DFT), a computational quantum mechanical modeling method.

Determination of photocatalytic activity

The photocatalytic activity of the synthesized NPs was evaluated by investigating the photocatalytic degradation of DR65 under UV-C light. Prior to examination of photocatalytic activity of the synthesized catalysts, effects of UV-C light without catalysts and adsorption of dye on surface catalysts were tested and decolorization ratio was monitored by UV–Vis spectrophotometry and TOC analysis. Photodegradation studies were performed in a solar box (Erichsen, model 1500) equipped with a Xe lamp with an efficient 675 W m^{-2}. Photocatalytic degradation conditions were determined by investigating parameters such as amount of catalyst (from 0.1 to 0.75 wt% in sol), irradiation time (1–4 h), and pH of medium (2–10). Photocatalytic degradation ratios of DR65 by the catalyst were determined using both a UV–Vis spectrophotometry (Varian Carry 50, λmax = 506 nm, dynamic calibration range of dye = 1–20 mg L-1; 0.0027–0.054 mM; R2 = 0.9973) and a total organic carbon analyzer (Teledyn Tekmar Torch TOC) at optimum conditions. In addition, the residual amount of DR65 in water at the optimum degradation conditions, before and after the photocatalytic degradation, was determined using an HPLC-equipped with a photodiode array detector (Thermo Finnigan model with FortisC_{18}; 150 × 4.6 mm separation column). The eluent was a mixture of acetonitrile and water (85%:15% *v*/*v*) and the elution was monitored at 506 nm at a flow rate of 1 mL/min, (dynamic calibration range of dye = 1–20 mg L^{-1}, R2 = 0.9998). To investigate intermediate products of DR65 after photodegradation, the eluent was mixed with acetonitrile and water (85%:15% *v*/*v*), and run on an LC-MS/MS-ESI (Agilent 6460 Triple Quad with Zorbax Eclipse Plus C18 Rapid Resolution) with separation column (flow rate 0.2 ml/min). Aqueous dispersions were prepared by adding the catalyst without FETAX solution or fish water to determine optimum degradation conditions of DR65. Then, the catalysts and DR65 were dispersed in FETAX solution or fish water and irradiated by UV-C light in solar box at the optimum conditions for use in toxicity studies. Samples were taken from the photoreaction apparatus at predetermined intervals and centrifuged after the photocatalytic degradation for all analytical measurements. Degradation ratio of DR65 in solution was calculated using the equation $(C_o\text{-}C_t/C_o) \times 100$, where C_0 is the initial concentrations and C_t are the residual concentrations at any time. All analytical methods were carried out in triplicate to obtain precise data.

Test organisms

Adult zebrafish colony (*Danio rerio*, Singapore type wild type) is grown and maintained in a Zebra fish Water System (ZebTec Active Blue, Tecniplast, Italy) in our laboratory. The

colony reproduced until F_3 generation and embryos of this population were used for all studies. The fish colony was maintained at 14:10 h light:dark photoperiod, pH 7.25 (± 0.15), conductivity 720 μS/cm (± 20), and 28.2 °C (± 0.2 °C). Fish were fed a 50:50 mixture of *Artemia* and *Spirulina* flakes (Bio-Marine Aquafauna, USA) twice daily and brine shrimp twice a week, ad libitum. Embryos were collected from an eight- to ten-months-old fish population in a spawning system (iSpawn, Tecniplast, Italy) within 3 h of laying, and their developmental stages were determined according to Kimmel et al. (1995). Embryos were kept in an incubator at 28.5 °C (± 0.1 °C) in standard embryo E2 medium (15 mM NaCl, 0.5 mM KCl, 1.0 mM $CaCl_2$, 0.15 mM KH_2PO_4, 0.05 mM Na_2HPO_4, 0.7 mM $NaHCO_3$, and 1.0 mM $MgSO_4$, pH 7.2) as described by Westerfield (2007) in petri dishes until 6–8 h post-fertilization (hpf). Zebrafish embryonic toxicity tests were performed in fish water using 60 mg L^{-1} NaCl in reverse osmosis water.

African clawed frog (*Xenopus laevis*) embryos were provided from our inbred colony according to methods described in Birhanli and Ozmen (2005). All fertilized frog eggs collected from the spawning tank were transferred into FETAX test solution (Dawson and Bantle 1987), which was used as a defined test medium for controls and as a diluent for exposures. Tests were performed as specified in the ASTM Standard Guide (2004). The FETAX solution has a conductivity of 1450 μS/cm at 21 °C. Jelly-coated embryos used for tests were visually inspected for normal development up to late-blastula stage (stage 8–11), at 5–6 hpf for experiments.

Toxicity tests for NPs

Single species toxicity tests were used to determine the adverse effects of NPs on zebrafish and *X. laevis* embryos. All acute toxicity tests were performed under static test conditions. The experiments for embryos were approved by the local ethical committee and conformed to the *Guide for the Care and Use of Laboratory Animals,* National Academy of Sciences, Washington, D.C. (NAS 1996). NPs were tested at 5, 25, 62.5, 125, and 250 mg L^{-1} concentrations according to preliminary experiments. Pure TiO_2 and SiO_2 NPs were also tested at the same concentrations.

NPs were dispersed by sonication for 30 min in fish water for all zebrafish tests and the zebrafish embryos were exposed to test solutions in 96 well microplates with 250 μL of solution, and an embryo that normally developed in each well was exposed. A minimum of 24 embryos was exposed to each concentration. pH was adjusted to 7.3 and conductivity was determined as approximately 700 μS/cm. The test nanomaterials to be used for the FETAX tests were dispersed in the FETAX solution with sonication for 30 min before being used in the *Xenopus* assays. Groups containing 4 embryos in each well of 24 well plates were tested with 8 well replicates containing 2 ml of test solutions. Thus, 32 embryos were used for each group in total. For zebrafish and *Xenopus* tests, the number of dead embryo or 1arvae was recorded, and remaining survivors at 96 h were anesthetized with MS-222 at 100 mg L^{-1} and evaluated for individual malformations by examining each specimen under a dissecting microscope (Harper et al. 2011). The zebrafish tests were maintained at 28.5 °C (± 0.1 °C) with 14:10 h light:dark photoperiod in an incubator, but *X. laevis* tests were performed at room temperature at 21.0 °C (± 1 °C) with 14:10 h light:dark photoperiod.

Photocatalytic degradation and toxicity tests

LC_{50} values for DR65 exposure were determined to identify initial dye concentration for photocatalytic degradation studies using species-specific test media as described above. Test organisms were also exposed to DR65 to obtain LC_{50}s for 24- to 96-h exposure periods according to the test species using species-specific test media as described above. LC_{50} values were determined for *D. rerio* and *X. laevis* embryos exposed from 8 to 96 hpf. For this aim, 0.95–50 mg L^{-1} and 0.95–14 mg L^{-1} concentrations of dye were tested on *D. rerio* and *X. laevis* embryos, respectively. After calculation of LC_{50}s, we decided to test photocatalytic degradation capability of synthesized NPs for 20 mg L^{-1} (0.054 mM) dye concentration that had extremely high toxicity for the test organisms. First, adsorption of DR65 on the NPs surface was determined. All degradation studies of DR65 were continued in distilled water under optimal pH conditions because fish water and FETAX medium caused a decrease in the photocatalytic degradation of dyes. However, animal testing was carried out after setting the medium pH to 7.2 or 7.4 and adding the necessary salts to adjust to the species specific test environment. Animals were evaluated for toxic effect of DR65 (20 mg L^{-1} stock) to detect the effect of degradation of DR65 without photocatalysts under UV-irradiation for up to 3 h. For this reason, test organisms were also exposed to UV-irradiated dye with NPs for 1–3 h. The decay of the dye was determined after exposure to UV for 3 h and the photocatalytic degradation was also monitored by chromatographic analysis.

Data analyses and statistics

LC_{50} values were calculated by Finney's Probit Analysis using software released by the EPA (Version 15.0). For developmental inhibition, data was assessed for normal distribution and homogeneity of variance by Sharipo–Wilks' test and Levene's test, respectively (SPSS software, Version 15.0; SPSS Inc., USA). Data with normal distribution and equal variance was analyzed by one-way ANOVA and independent sample *t* test. Data that did not meet the assumptions required for parametric testing were analyzed using a Kruskal–Wallis test and the Mann–Whitney *U* test.

Results and discussion

NP characterization

Figure 1 shows a typical SEM and TEM microphotograph of the synthesized NPs indicating that the shapes of the particles are predominantly spherical. In addition, all the products prepared are heterogeneous and the coatings are not uniform. This may be due to the aggregation of TiO_2 colloid particles and the formation of larger particles. A nonuniform distribution of coated particles was observed which consisted of either some single particles or a cluster of particles. All SiO_2@TiO_2 CS structures have a rough and textured surface. Table 1 presents the elemental composition of all synthesized NPs, which were analyzed by energy dispersive x-ray (EDX) spectroscopy. The results show partial TiO_2 deposit on SiO_2 core and SiO_2 deposit on TiO_2 core.

Figure 2a represents the characterization of the pure TiO_2, SiO_2, and the novel CS NPs. According to XRD model data, it is understood that all NPs except SiO_2 are in anatase structure. It can be concluded that the slight decrease in diameter of SiO_2@TiO_2 CS NPs compared to SiO_2 comes from TiO_2 coating on the surface of SiO_2 NP. The coating procedure caused an increased peak intensity of anatase but the width of the peak (101) becomes narrower for TiO_2-coated SiO_2 due to the increased grain size. On the other hand, Fig. 2b shows that dispersion of the NPs was bimodal in water after sonication. The crystallite sizes of synthesized NPs were calculated by applying the Scherrer equation estimation from anatase (101) plane diffraction peak ($2\theta = 25.4^{o}$) and the main particle size distributions in water were analyzed using DLS measurements. The average size of the primary particles was 11.5 nm, 15.3 nm, 16.2 nm, and 11 nm for TiO_2, SiO_2@TiO_2, SiO_2, and TiO_2@SiO_2, respectively. The Brunauer–Emmett–Teller surface area (S_{BET}) values were determined as 249.5, 167.6, 184.8, and 83.0 $m^2\ g^{-1}$ for the all NPs, respectively (Table 2). The specific surface area is one of the important parameters to be considered for photocatalytic activity. As shown in Table 2, BET surface areas of coated NPs were obviously lower than pure TiO_2 or SiO_2 due to coating effects. It was observed that the photocatalytic capability of SiO_2@TiO_2 NP on DR65 decreased relatively to pure TiO_2 based on BET surface area. In any case, pure SiO_2 and TiO_2@SiO_2 NP had low photocatalytic effects on DR65, likely due to their crystallite size (Hou et al. 2015).

Figure 3a shows FTIR patterns of pure and coated NPs. The broad peaks centered at 3420.68 and 1630.39 cm^{-1} are associated with O-H and H-O-H bending vibration. The peaks at 1099.96, 807.47, and 467 belong to the asymmetric (Si-O-Si) stretching vibration, the symmetric (Si-O-Si) stretching vibration, and the Si-O-Si band, respectively. The Si-O-Si peak at 467.12 coincides with the Ti-O-Ti band. The peak in 959.40 corresponds to the Ti-O-Si vibration (Falahatdoost et al. 2015). Since the surface charge of the photocatalyst plays an important role in photocatalytic processes, the environmental pH value is also important in measurements. For this reason, the obtained data was determined at optimum pH conditions for the study and found to be compatible with our expectations. The iso-electric point (ISE) defines the pH range at which the surface is neutrally charged. Figure 3b shows the variation of zeta potential with pH for the synthesized NPs. The variations give an isoelectric point (ISE) at pH 3 for SiO_2 particles, at pH 2 for TiO_2@SiO_2, at pH 4.97 for TiO_2, and at pH 6.05 for SiO_2@TiO_2. It is clear that titania coating on silica particles has increased the electrophoretic mobility and zeta potential

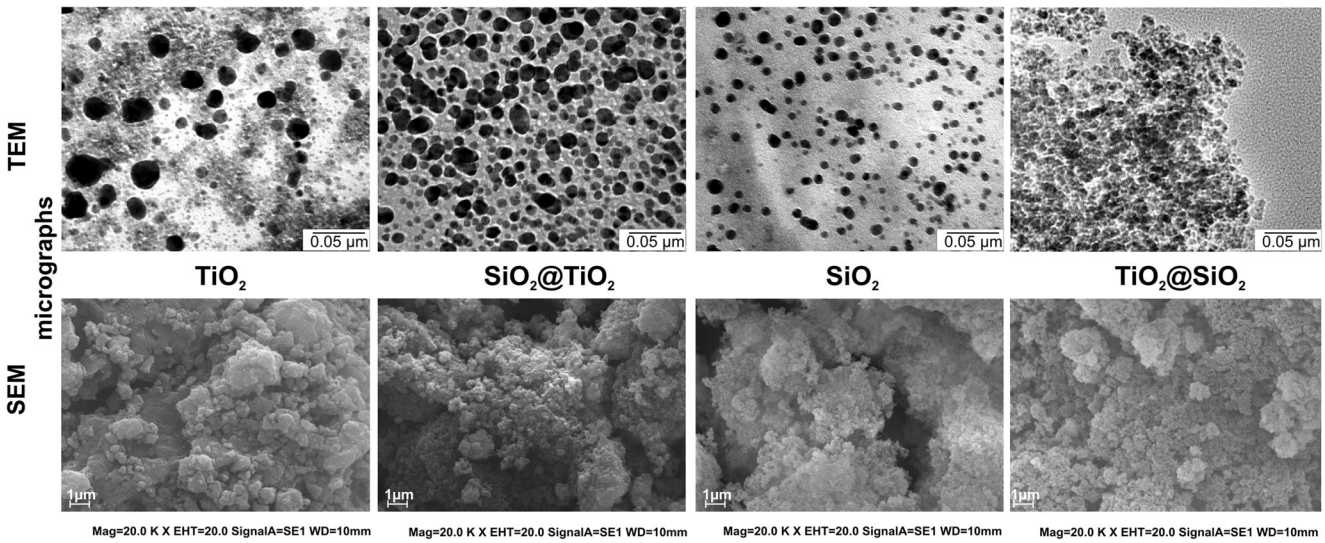

Fig. 1 SEM and TEM micrographs of the synthesized NPs

Table 1 Energy dispersive x-ray results on the elemental composition of the synthesized NPs

Element	Atomic concentration (a.t.%)			
	TiO_2	SiO_2@TiO_2	SiO_2	TiO_2@SiO_2
Ti	31.37	12.67	–	12.28
O	68.63	77.49	87.04	73.11
Si	–	9.04	12.96	14.61

Table 2 Crystallite size, particle size distribution in water, and specific surface area of the synthesized NPs

Material	Crystallite size (nm)	Particle size distribution (nm)	S_{BET} (m^2 g^{-1})
TiO_2	11.5	220; 825	249.49
SiO_2@TiO_2	15.3	220; 955	167.66
SiO_2	16.2	255; 2304	184.78
TiO_2@SiO_2	11.0	255; 1106	82.99

values of + 30 mV and − 30 mV in acidic and basic medium, respectively. The surface charge also affects the adsorption process of organic molecule on the surface of photocatalysts (Ullah et al. 2015).

Photocatalytic degradation of DR65

It is well known that many of the azo dyes are toxic and genotoxic for organisms after biotransformation. They may also have ecotoxicological risks for aquatic ecosystems (Abe et al. 2017; Chequer et al. 2009; Chequer et al. 2011). One of the commonly used azo dyes is disperse red 65 selected to determine the photocatalytic degradation capacity of core@shell NPs in this work. According to our preliminary studies, the degradation rate of DR65 was about 16.5% after 180 min of exposure based on UV-C irradiation results without photocatalyst of DR65 and its toxicity on test organisms was still very high. Hence, high dye concentration (20 mg L^{-1}) has been tested in evaluating photocatalytic degradation capacity and toxic efficacy of synthesized nanomaterials.

Adsorption of the dye on the surface of the photocatalysts may cause reduction of the toxicity and therefore adsorption capacity of synthesized NPs was also tested. The adsorption-desorption equilibriums for the concentration of the studied dyes are summarized in Table 3. It has been found that pure SiO_2 and TiO_2 have a high adsorption capacity for DR65 and SiO_2 or TiO_2 NPs can adsorb more than 40% of the dye in 60 min. However, the adsorption of the dye with synthesized CS NPs was determined to be about 17% and 32% for SiO_2@TiO_2 and TiO_2@SiO_2, respectively. On the other hand, neither UV-C irradiation nor dye adsorption was completely effective in removing DR65 from the water. Accordingly, the dye concentration is still high in water in terms of toxicity. For this reason, it is also important to evaluate the degradation of the dye concentration at the toxic level in water by the synthesized photocatalytic material. The photocatalytic degradation ratios determined using synthesized NPs are given in Table 4. According to this, it was determined that the dyes exposed to UV-C effect for 3 h could be degraded 98% with TiO_2 and $Si0_2$@TiO_2 catalysts. However, SiO_2 and TiO_2@SiO_2 NPs photocatalytically degraded DR65 at only about 5% and 18%, respectively, under UV-C irradiation (Table 4). Additionally, it was found that degradation considerably decreased in alkaline pH. This effect in alkaline conditions may be explained by the chemical state of TiO_2 on the surface and ionization of DR65 under alkaline conditions. As shown in Fig. 3b, the iso-electric point (ISE) of the NPs was determined at pH 4.97 and at 6.05 for pure TiO_2 and SiO_2@TiO_2, respectively. However,

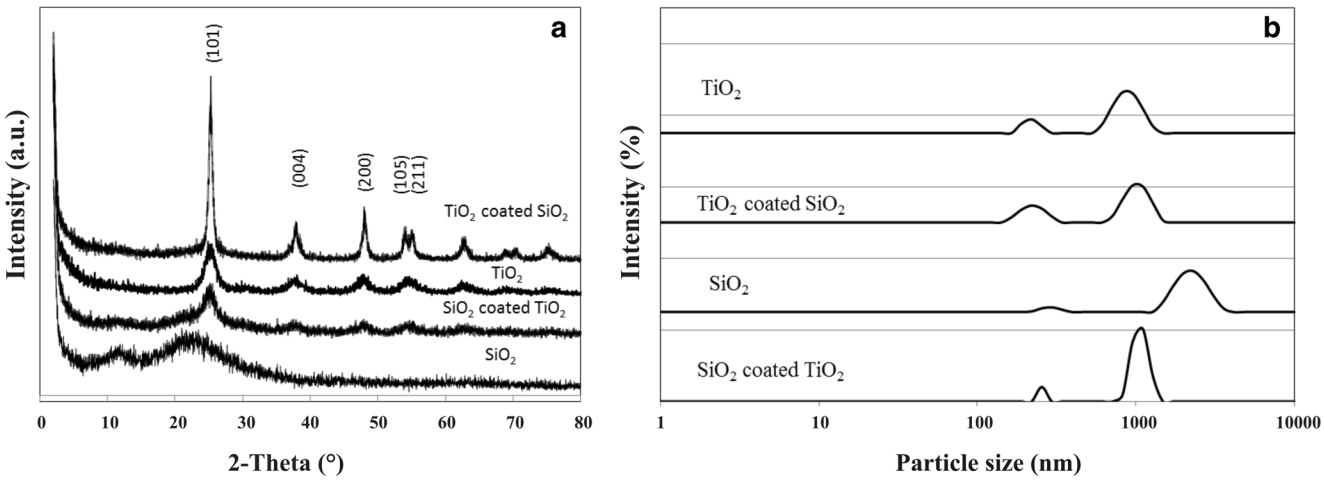

Fig. 2 XRD patterns of the synthesized NPs (**a**) and particle size distribution in water (**b**)

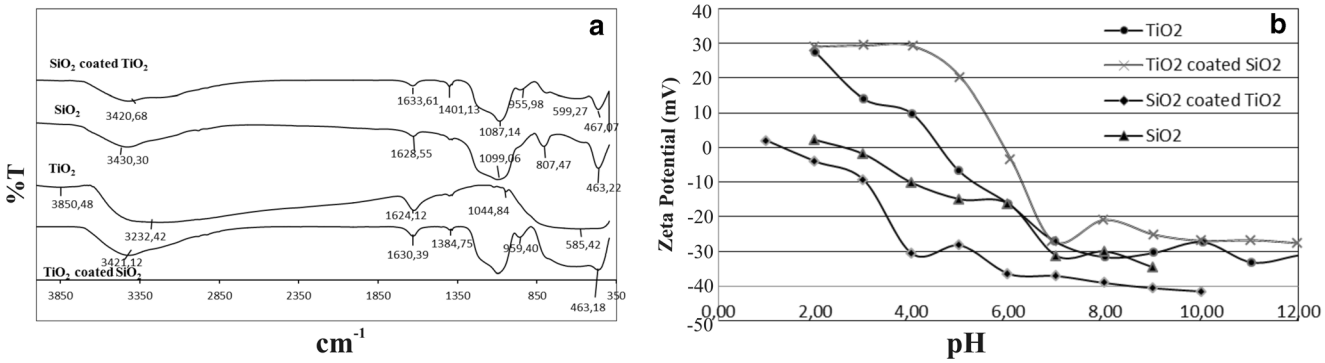

Fig. 3 FTIR spectra (**a**) and zeta potentials (**b**) of the synthesized NPs

Table 3 Adsorption ratios of DR65 on surface of synthesized NPs (0.3% wt/v in sol) according to UV–Vis spectrophotometric analysis ($X_{mean} \pm$ S.D.; $n = 3$)

Time (min)	Adsorption (%)			
	SiO_2 (pH:7.1)	TiO_2 (pH:3.30)	TiO_2@SiO_2 (pH: 6.9)	SiO_2@TiO_2 (pH:4.64)
5	31.0 ± 2.2	51.4 ± 3.2	26.3 ± 2.8	1.0 ± 0.4
15	40.0 ± 3.1	33.8 ± 2.9	35.7 ± 3.3	22.3 ± 2.3
30	43.1 ± 4.3	35.6 ± 2.8	33.9 ± 3.2	16.4 ± 2.1
45	45.7 ± 4.4	42.0 ± 3.0	31.0 ± 3.2	16.0 ± 2.2
60	44.4 ± 4.3	41.0 ± 3.1	32.3 ± 3.4	17.2 ± 2.4

S.D. standard deviation, *n* the number of replicates

the surface of NPs becomes negatively charged at high pH values. It is well known that photocatalytic degradation of dyes are affected by several parameters such as oxidizing agents, pH, dye concentration, type, and concentration of photocatalysts (Hung and Yuan 2000; Li et al. 2003; Poulios et al. 2000; Qamar et al. 2005; Saggioro et al. 2011; Wang et al. 2008). Thus, all degradation studies were conducted in distilled water and under optimal pH conditions as mentioned by Reza et al. (2017), and the highest rate of degradation was reached after 180 min UV-C exposure periods (Table 5). However, the environmental conditions were arranged according to the fish water or FETAX solution specifications before toxicity assays.

Degradation products formed at the end of the irradiation process were analyzed by LC/MS/MS and identified by interpretation of their mass spectra data representing their molecular ion peaks with respect to *m/z*. The main species detected in the solutions are presented in Fig. 4 along with LC/MS/MS spectra for the aqueous solutions of 20 mg L^{-1} of DR65, under UV-C after 180 min photolysis with the absence of catalyzer. The main peak was observed in 371.800 *m/z* at the beginning of analysis in water (Fig. 4a). However, the highest peak was not present as a result of irradiation of DR65 under UV-C for 180 min. This can be regarded as a sign of successful dye degradation. However, this finding was also supported by toxicity assays.

Table 4 Photocatalytic degradation ratios of DR65 within 180 min for the all synthesized NPs for the toxicity studies ($X_{mean} \pm$ S.D.; $n = 3$)

Methods	Degradation (%)			
	SiO_2	TiO_2	TiO_2@SiO_2	SiO_2@TiO_2
UV/Vis spect.	5.09 ± 1.10	94.7 ± 4.10	18.7 ± 1.20	92.5 ± 5.30
TOC	4.00 ± 1.80	90.1 ± 3.44	19.2 ± 1.40	85.8 ± 2.05
HPLC-DAD	4.80 ± 1.20	99.7 ± 0.85	18.0 ± 0.90	97.5 ± 0.92

S.D. standard deviation, *n* the number of replicates

Toxicity tests

Core- and shell-structured NPs may have some advantages over simple NPs as a result of improving properties such as distributability, conjugation with biomolecules, and thermal and chemical stability (Chatterjee et al. 2014). The toxicity of metal-based NPs may depend on the ions released from the NPs, some of their physical and/or chemical properties or environmental conditions (Devin et al. 2017). However, the core/shell structure can make nano-materials more biocompatible and may change into environmentally safer structures (Aillon et al. 2009; Sounderya and Zhang 2008). Sometimes the shell layer cannot only act as a nontoxic layer,

Table 5 Effect of irradiation time on photodegradation of DR65 with TiO_2 and TiO_2-coated SiO_2 at the optimum conditions (X_{mean} ± S.D.; $n = 3$)

Time, min	Degradation (%)					
	TiO_2			$SiO_2@TiO_2$		
	UV–Vis spect.	TOC	HPLC-DAD	UV–Vis spect.	TOC	HPLC-DAD
60	92.48 ± 1.04	20.75 ± 2.13	1.09 ± 0.70	27.33 ± 2.52	52.99 ± 3.46	4.17 ± 1.65
120	91.73 ± 2.10	37.78 ± 3.45	39.98 ± 1.23	82.01 ± 1.79	63.59 ± 2.33	33.50 ± 2.24
180	94.70 ± 4.10	90.08 ± 3.44	99.7 ± 0.85	92.51 ± 5.30	85.80 ± 2.05	97.54 ± 0.92

S.D. standard deviation, *n* the number of replicates

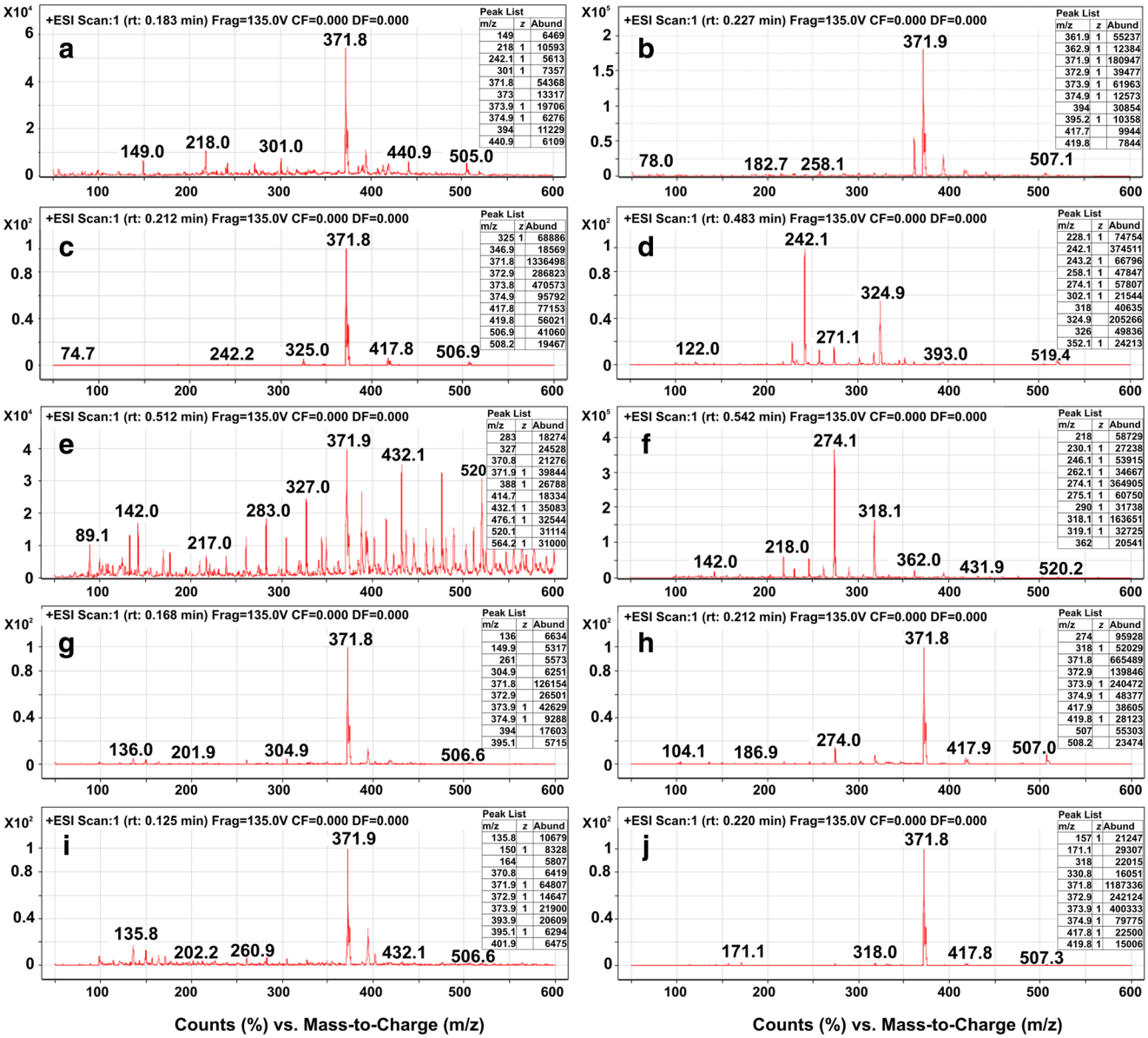

Fig. 4 Analysis of intermediates formed by degradation of DR65 using UV radiation and/or combined treatment of synthesized NPs. **a** Initial assay of DR65 in water; **b** irradiated DR65 under UV-C; **c** initial assay of DR65 with TiO_2; **d** irradiated DR65 with TiO_2; **e** initial assay of DR65 with $SiO_2@TiO_2$; **f** irradiated DR65 with $SiO_2@TiO_2$; **g** initial assay of DR65 with SiO_2; **h** irradiated DR65 with SiO_2; **i** initial assay of DR65 with $TiO_2@SiO_2$; **j** irradiated DR65 with $TiO_2@SiO_2$

Table 6 Evaluation of the toxic effect of the textile dye DR65 on embryos after 1–3 h photocatalytic degradation with synthesized NPs

Catalyst	Lethality (%)							
	X. laevis				*D. rerio*			
	0 h	1 h	2 h	3 h	0 h	1 h	2 h	3 h
Control	0	0	0	0	0	0	0	0
SiO_2	100	100	3.1	0	100	100	91.7	8.3
TiO_2@SiO_2	100	100	28.1	0	100	100	100	0
TiO_2	100	100	3.1	0	100	95.8	100	4.2
SiO_2@TiO_2	100	100	25	0	100	95.8	79.2	4.2

but may also improve the desired properties of the core material. Semiconductor CS NPs can improve the optical properties, photostability, and hydrophobicity of other materials incorporated into the structure. On the other hand, silica is one of the best materials with a rich and well-known surface chemistry, adsorption capacity, optical clarity, and mechanical stability and is low cost in the preparation of CS NPs (Li et al. 2017). Therefore, there are many reports in literature on SiO_2@TiO_2 CSNPs prepared by sol-gel, hydrothermal, reflux, impregnation, and precipitation methods (Ullah et al. 2015; Zhao et al. 2005).

The core structure of the novel TiO_2 NPs was able to reduce more than 90% of the azo dye in the water environment according to the photocatalytic studies. Most importantly, even the highest test concentration of CS NPs (250 mg L^{-1}) did not cause significant mortality (little mortality was observed) when compared to control groups in *D. rerio* and *X. laevis* embryos. The lower concentrations of NPs did not cause lethality to the embryos of the model organisms. Furthermore, the synthesized CS NPs did not cause embryonic developmental abnormalities during 96 hpf for either *D. rerio* and *X. laevis*.

A series of DR65 concentrations ranging from 5 to 125 mg L^{-1} were tested and 100% mortality was observed within 48 h after exposure to the dye in fish water, indicating that it is very toxic to the test organisms. On the other hand, after 96 h of exposure, the LC_{50}s were calculated as 1.37 mg L^{-1} (CI: 1.15–1.56 (0.0037 mM) for *D. rerio* and 4.67 mg L^{-1} (CI: 4.40–4.99) (0.013 mM) for *X. laevis* embryos.

Due to our preliminary studies mentioned above and high toxicity risk of DR65, we preferred to test 20 mg L^{-1} dye concentration for all degradation studies. This concentration is 4 and 15 times higher than the LC_{50}s calculated for *D. rerio* and *X. laevis*, respectively. On the other hand, it has been found that exposure to UV-C without NP catalysts for 1 to 3 h did not remove the toxicity and the lethal effect continued for both frog and zebrafish embryos. These findings were also supported by LC/MS/MS results (Fig. 4). Therefore, photocatalytic application of titanium-based CS NPs may provide an alternative for this purpose, as UV-C irradiation was not sufficiently effective for treatment of wastewater containing DR65. Accordingly, toxicity tests were carried out in subsequent studies using a solution that appeared as a sample of photocatalytic degradation of the dye. In dye degradation studies, frog embryos showed better tolerance to higher dye concentrations than fish embryos. However, it should be noted that the dye concentration chosen for our photocatalytic degradation studies is a more significant environmental contaminant in the water ecosystem than expected.

Nonetheless, exposure to photocatalytically degraded DR65 for 1 h with synthesized NPs resulted in 100% death after 96 h of exposure in both test organisms, while photocatalytic degradation for 2 h was able to partially mitigate the

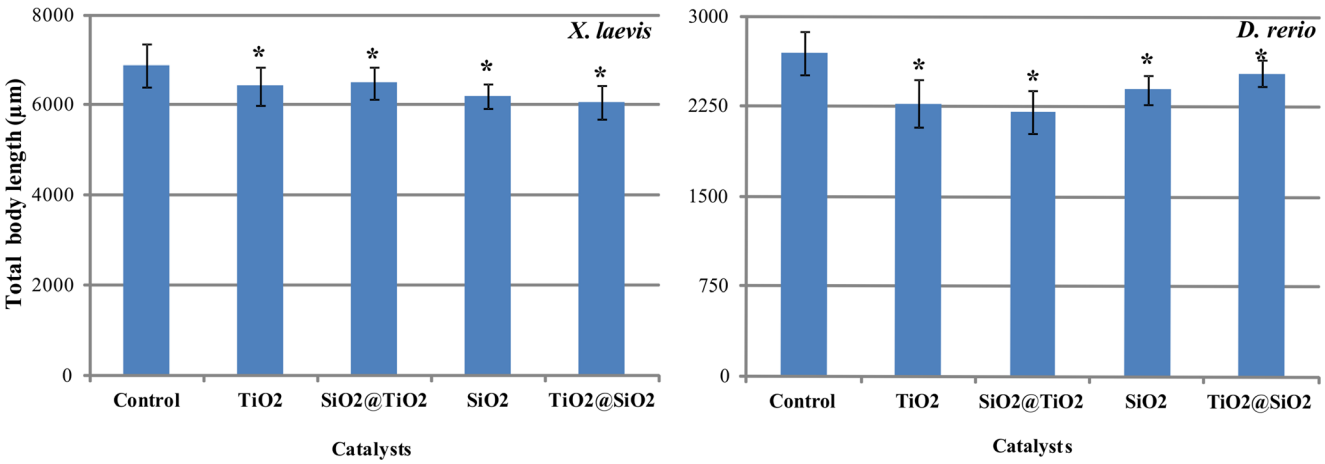

Fig. 5 Developmental inhibition of *X. laevis* and *D. rerio* embryos exposed to DR65 subjected to photocatalytic degradation with each of the synthesized catalysts for 3 h. Independent Samples Test or Mann–Whitney *U* test performed to compare results against control embryos for statistical significance (*$p < 0.001$)

lethal effect for *X. laevis* embryos. Furthermore, the photocatalytically degraded dye for 3 h did not cause mortality in *X. laevis* embryos (Table 6). Similar results were also observed for *D. rerio* embryos such that 3-h photocatalytic degradation of the dye with TiO_2 and SiO_2@TiO_2 catalysts removed the lethal effects of DR65 on zebrafish embryos. However, it has been found that dye degradation could not completely remove the toxic effect on fish embryos and can lead to a decrease in lethal effect. Fish embryos, which continued to develop at 28.5 °C, could not exit the chorionic membrane within 48–72 h. The surviving embryos showed significant developmental delays and their total body length significantly decreased compared with control embryos ($p < 0.001$) for both frog and zebrafish (Fig. 5). These results demonstrate that photocatalytic degradation could not remove the toxic effects of DR65 with new NPs completely and that ecotoxicological risk continued.

The use of binary metal oxides as photocatalysts is not a completely new approach. Kwon et al. (2000) have published the results on TiO_2/WO_3 composites as photocatalysts for photooxidation of 1,4-dichlorobenzene. Researchers found that the degradation rates of 1,4-dichlorobenzene were increased about three times. They have also found a strong correlation between surface acidity and reactivity. Recently, Khataee et al. (2009), Zhang et al. (2010), Sun et al. (2012), Ozmen et al. (2015), and Lakshmi and Rajagopalan (2016) published photocatalytic activities of different type of nano-composite materials for degradation of different types of dyes under visible light or UV exposure. Furthermore, Zhang et al. (2016), Farhadi et al. (2017), You et al. (2017), and Milenova et al. (2017) published on the photocatalytic activities of CS NPs on degradation of different azo dyes. However, the evaluation of the toxic effects of xenobiotic by-products, which are photocatalytically degraded by CS NPs, is rather limited in the literature. The toxicity testing of photocatalytic by-products are also important for synthesis of eco-friendly novel nano-materials. Finally, we have produced new CS NPs to address the toxicity of photocatalytically degraded azo dye and have evaluated the effects on different aquatic environments in this study.

Conclusions

The novel TiO_2-SiO_2 nano-structures were characterized using TEM and SEM microscopy, crystal size, zeta potential, X-Ray diffraction, FTIR investigation, and specific surface area of the particles. According to characterization studies, it has been determined that these core@shell nano-composite materials synthesized by the reflux method have a homogeneous structure. The photocatalytic activities and adsorption capacity of CS NPs with UV-C irradiation were evaluated using reference azo dye DR65. Our novel CS NPs slightly absorbed the dye, but the remaining concentration was still very high. Toxicity of NPs was assessed by exposure to NPs during early developmental stages of *Xenopus laevis* and *Danio rerio* embryos. Accordingly, the effects of lethality and development of malformations were evaluated. Photocatalytic degraded DR65 by-products were evaluated to determine the ecotoxicological risk of NP-pollutant interactions. Low toxic effects determined for the aquatic test animals reveal that fabrication of CS NPs may have some advantages over pure NPs; for example, photocatalytic methods can be used effectively to reduce the adverse effects of environmental contaminants such as toxic azo dyes in wastewater. The results of the study showed that UV-C irradiation alone did not remove the lethal effects of the dye, but mortality was reduced when DR65 was exposed to NPs with UV-C radiation for 3 h. However, significant toxicity symptoms were still observed in exposed embryos.

Funding information The financial supports as bilateral collaborative project from The Scientific and Technological Research Council of Turkey (TÜBİTAK) (grant no.: 113Z561) and National Science Foundation in the USA (grant no.: 1438165) are gratefully acknowledged.

References

Abe FR, Mendonca JN, Moraes LA, Oliveira GA, Gravato C, Soares AM, Oliveira DP (2017) Toxicological and behavioral responses as a tool to assess the effects of natural and synthetic dyes on zebrafish early life. Chemosphere 178:282–290

Aillon KL, Xie YM, El-Gendy N, Berkland CJ, Forrest ML (2009) Effects of nanomaterial physicochemical properties on in vivo toxicity. Adv Drug Deliver Rev 61:457–466

ASTM (American Society for Testing and Materials) (2004) ASTM standard guide for conducting the Frog Embryo Teratogenesis Assay–Xenopus (FETAX). E1439–98. American Society for Testing and Materials. vol. 11.05, Philadelphia

Birhanli A, Ozmen M (2005) Evaluation of the toxicity and teratogenity of six commercial textile dyes using the frog embryo teratogenesis assay-Xenopus. Drug Chem Toxicol 28:51–65

Burello E (2015) Computational design of safer nanomaterials. Environ Sci-Nano 2:454–462

Caruso RA, Susha A, Caruso F (2001) Multilayered titania, silica, and Laponite nanoparticle coatings on polystyrene colloidal templates and resulting inorganic hollow spheres. Chem Mater 13:400–409

Chatterjee K, Sarkar S, Jagajjanani Rao K, Paria S (2014) Core/shell nanoparticles in biomedical applications. Adv Colloid Interf Sci 209:8–39

Chequer FM, Angeli JP, Ferraz ER, Tsuboy MS, Marcarini JC, Mantovani MS, de Oliveira DP (2009) The azo dyes disperse red 1 and disperse orange 1 increase the micronuclei frequencies in human lymphocytes and in HepG2 cells. Mutat Res 676:83–86

Chequer FM, Lizier TM, de Felicio R, Zanoni MV, Debonsi HM, Lopes NP, Marcos R, de Oliveira DP (2011) Analyses of the genotoxic and mutagenic potential of the products formed after the biotransformation of the azo dye disperse red 1. Toxicol in Vitro 25:2054–2063

Clemente Z, Castro VLSS, Moura MAM, Jonsson CM, Fraceto LF (2014) Toxicity assessment of TiO_2 nanoparticles in zebrafish

embryos under different exposure conditions. Aquat Toxicol 147: 129–139
Dawson DA, Bantle JA (1987) Development of a reconstituted water medium and preliminary validation of the frog embryo teratogenesis assay Xenopus (Fetax). J Appl Toxicol 7:237–244
Demirors AF, van Blaaderen A, Imhof A (2009) Synthesis of eccentric titania-silica core-shell and composite particles. Chem Mater 21: 979–984
Devin S, Buffet PE, Chatel A, Perrein-Ettajani H, Valsami-Jones E, Mouneyrac C (2017) The integrated biomarker response: a suitable tool to evaluate toxicity of metal-based nanoparticles. Nanotoxicology 11:1–6
Falahatdoost S, Ara MHM, Shaban Z, Ghazyani N (2015) Optical investigation of shell thickness in light scattering SiO_2 particle with TiO_2 nanoshells and its application in dye sensitized solar cells. Opt Mater 47:51–55
Farhadi A, Mohammadi MR, Ghorbani M (2017) On the assessment of photocatalytic activity and charge carrier mechanism of TiO_2@SnO_2 core-shell nanoparticles for water decontamination. J Photoch Photobio A 338:171–177
Faria M, Navas JM, Raldua D, Soares AM, Barata C (2014) Oxidative stress effects of titanium dioxide nanoparticle aggregates in zebrafish embryos. Sci Total Environ 470-471:379–389
Fujiwara K, Kuwahara Y, Sumida Y, Yamashita H (2017) Controlling photocatalytic activity and size selectivity of TiO_2 encapsulated in hollow silica spheres by tuning silica shell structures using sacrificial biomolecules. Langmuir 33:6314–6321
Garcia-Alonso J, Rodriguez-Sanchez N, Misra SK, Valsami-Jones E, Croteau MN, Luoma SN, Rainbow PS (2014) Toxicity and accumulation of silver nanoparticles during development of the marine polychaete Platynereis dumerilii. Sci Total Environ 476-477:688–695
Gramowski A, Flossdorf J, Bhattacharya K, Jonas L, Lantow M, Rahman Q, Schiffmann D, Weiss DG, Dopp E (2010) Nanoparticles induce changes of the electrical activity of neuronal networks on microelectrode array neurochips. Environ Health Perspect 118:1363–1369
Gupta S, Tripathi M (2011) A review of TiO_2 nanoparticles. Chin Sci Bull 56:1639–1657
Habibi MH, Bagheri P (2017) Enhanced photo-catalytic degradation of naphthol blue black on nano-structure $MnCo_2O_4$: charge separation of the photo-generated electron-hole pair. J Mater Sci-Mater El 28: 289–294
Hariharan C (2006) Photocatalytic degradation of organic contaminants in water by ZnO nanoparticles: revisited. Appl Catal a-Gen 304:55–61
Harper SL, Carriere JL, Miller JM, Hutchison JE, Maddux BLS, Tanguay RL (2011) Systematic evaluation of nanomaterial toxicity: utility of standardized materials and rapid assays. ACS Nano 5:4688–4697
Hou LR, Hua H, Cao H, Zhu SQ, Yuan CZ (2015) A core-shell TiO_2@C nano-architecture: facile synthesis, enhanced visible photocatalytic performance and electrochemical capacitance. RSC Adv 5:62424–62432
Hu Y, Tsai HL, Huang CL (2003) Phase transformation of precipitated TiO_2 nanoparticles. Mat Sci Eng a-Struct 344:209–214
Hung CH, Yuan C (2000) Reduction of azo-dye via TiO_2-photocatalysis. J Chin Inst Environ Eng 10:209–216
Ijadpanah-Saravi H, Zolfaghari M, Khodadadi A, Drogui P (2016) Synthesis, characterization, and photocatalytic activity of TiO_2-SiO_2 nanocomposites. Desalin Water Treat 57:14647–14655
Jovanovic B (2015) Critical review of public health regulations of titanium dioxide, a human food additive. Integr Environ Assess Manag 11:10–20
Khan SA, Jensen KF (2007) Microfluidic synthesis of titania shells on colloidal silica. Adv Mater 19:2556–2560
Khataee AR, Pons MN, Zahraa O (2009) Photocatalytic degradation of three azo dyes using immobilized TiO_2 nanoparticles on glass plates activated by UV light irradiation: influence of dye molecular structure. J Hazard Mater 168:451–457
Kimmel CB, Ballard WW, Kimmel SR, Ullmann B, Schilling TF (1995) Stages of embryonic-development of the zebrafish. Dev Dynam 203:253–310
Kwon YT, Song KY, Lee WI, Choi GJ, Do YR (2000) Photocatalytic behavior of WO_3-loaded TiO_2 in an oxidation reaction. J Catal 191: 192–199
Lakshmi PV, Rajagopalan V (2016) A new synergetic nanocomposite for dye degradation in dark and light. Sci Rep-Uk 6:38606
Lee JW, Kong S, Kim WS, Kim J (2007) Preparation and characterization of SiO_2/TiO_2 core-shell particles with controlled shell thickness. Mater Chem Phys 106:39–44
Li L, Zhu W, Zhang P, Chen Z, Han W (2003) Photocatalytic oxidation and ozonation of catechol over carbon-black-modified nano-TiO_2 thin films supported on Al sheet. Water Res 37:3646–3651
Li JF, Zhang YJ, Ding SY, Panneerselvam R, Tian ZQ (2017) Core-shell nanoparticle-enhanced Raman spectroscopy. Chem Rev 117:5002–5069
Milenova K, Zaharieva K, Stambolova I, Blaskov V, Eliyas A, Dimitrov L (2017) Photocatalytic performance of TiO_2 , CeO_2, ZnO and TiO_2 -CeO_2 -ZnO in the course of methyl orange dye degradation. J Chem Technol Metallurgy 52:13–19
Moore MN (2006) Do nanoparticles present ecotoxicological risks for the health of the aquatic environment? Environ Int 32:967–976
Mueller NC, Nowack B (2008) Exposure modeling of engineered nanoparticles in the environment. Environ Sci Technol 42:4447–4453
NAS (1996) National Academy of Sciences. Guide for the Care and Use of Laboratory Animals. National Research Council, Institute for Laboratory Animal Research, Washington, D.C. http://www.nap.edu/catalog/5140.html
Ni M, Leung MKH, Leung DYC, Sumathy K (2007) A review and recent developments in photocatalytic water-splitting using TiO_2 for hydrogen production. Renew Sust Energ Rev 11:401–425
Nogueira V, Lopes I, Rocha-Santos TAP, Rasteiro MG, Abrantes N, Goncalves F, Soares AMVM, Duarte AC, Pereira R (2015) Assessing the ecotoxicity of metal nano-oxides with potential for wastewater treatment. Environ Sci Pollut R 22:13212–13224
Ostaszewska T, Chojnacki M, Kamaszewski M, Sawosz-Chwalibog E (2016) Histopathological effects of silver and copper nanoparticles on the epidermis, gills, and liver of Siberian sturgeon. Environ Sci Pollut R 23:1621–1633
Ozmen M, Gungordu A, Erdemoglu S, Ozmen N, Asilturk M (2015) Toxicological aspects of photocatalytic degradation of selected xenobiotics with nano-sized Mn-doped TiO_2. Aquat Toxicol 165:144–153
Pan X, Zhao Y, Liu S, Korzeniewski CL, Wang S, Fan ZY (2012) Comparing graphene-TiO_2 nanowire and graphene-TiO_2 nanoparticle composite photocatalysts. Acs Appl Mater Inter 4:3944–3950
Poulios I, Avranas A, Rekliti E, Zouboulis A (2000) Photocatalytic oxidation of auramine O in the presence of semiconducting oxides. J Chem Technol Biot 75:205–212
Qamar M, Saquib M, Muneer M (2005) Photocatalytic degradation of two selected dye derivatives, chromotrope 2B and amido black 10B, in aqueous suspensions of titanium dioxide. Dyes Pigments 65:1–9
Reza KM, Kurny ASW, Gylshan F (2017) Parameters affecting the photocatalytic degradation of dyes using TiO_2: a review. Appl Water Sci 7:1569–1578
Robert D, Keller N, Selli E (2017) Environmental photocatalysis and photochemistry for a sustainable world: a big challenge. Environ Sci Pollut Res Int 24:12503–12505
Saggioro EM, Oliveira AS, Pavesi T, Maia CG, Ferreira LFV, Moreira JC (2011) Use of titanium dioxide photocatalysis on the remediation of model textile wastewaters containing azo dyes. Molecules 16: 10370–10386

Shanmugam S, Gabashvili A, Jacob DS, Yu JC, Gedanken A (2006) Synthesis and characterization of TiO_2@C core-shell composite nanoparticles and evaluation of their photocatalytic activities. Chem Mater 18:2275–2282

Shiba K, Takei T, Ogawa M (2016) Mesoporous silica coated silica-titania spherical particles: from impregnation to core-shell formation. Dalton T 45:18742–18749

Sonune A, Ghate R (2004) Developments in wastewater treatment methods. Desalination 167:55–63

Sounderya N, Zhang Y (2008) Use of core/shell structured nanoparticles for biomedical applications. Recent Pat Biomed Eng 1:34–42

Sun M, Chen GD, Zhang YK, Wei Q, Ma ZM, Du B (2012) Efficient degradation of azo dyes over Sb_2S_3/TiO_2 heterojunction under visible light irradiation. Ind Eng Chem Res 51:2897–2903

Ullah S, Ferreira-Neto EP, Pasa AA, Alcantara CCJ, Acuna JJS, Bilmes SA, Ricci MLM, Landers R, Fermino TZ, Rodrigues UP (2015) Enhanced photocatalytic properties of core@shell SiO_2@TiO_2 nanoparticles. Appl Catal B-Environ 179:333–343

Wang N, Li J, Zhu LH, Dong Y, Tang HQ (2008) Highly photocatalytic activity of metallic hydroxide/titanium dioxide nanoparticles prepared via a modified wet precipitation process. J Photoch Photobio A 198:282–287

Westerfield M (2007) The zebrafish book, 5th edition; a guide for the laboratory use of zebrafish (*Danio rerio*). University of Oregon Press, Eugene

Westerhoff P, Song GX, Hristovski K, Kiser MA (2011) Occurrence and removal of titanium at full scale wastewater treatment plants: implications for TiO_2 nanomaterials. J Environ Monitor 13:1195–1203

Yang Y, Wang H, Li J, He B, Wang T, Liao S (2012) Novel functionalized nano-TiO_2 loading electrocatalytic membrane for oily wastewater treatment. Environ Sci Technol 46:6815–6821

You H, Wu Z, Jia Y, Xu X, Xia Y, Han Z, Wang Y (2017) High-efficiency and mechano-/photo- bi-catalysis of piezoelectric-ZnO@ photoelectric-TiO_2 core-shell nanofibers for dye decomposition. Chemosphere 183:528–535

Zhang J, Xu Q, Feng Z, Li M, Li C (2008) Importance of the relationship between surface phases and photocatalytic activity of TiO_2. Angew Chem Int Edit 47:1766–1769

Zhang H, Chen D, Lv XJ, Wang Y, Chang HX, Li JH (2010) Energy-efficient photodegradation of azo dyes with TiO_2 nanoparticles based on photoisomerization and alternate UV-visible light. Environ Sci Technol 44:1107–1111

Zhang Y, Gao F, Wanjala B, Li ZY, Cernigliaro G, Gu ZY (2016) High efficiency reductive degradation of a wide range of azo dyes by SiO_2-Co core-shell nanoparticles. Appl Catal B-Environ 199:504–513

Zhao L, Yu JG, Cheng B (2005) Preparation and characterization of SiO_2/TiO_2 composite microspheres with microporous SiO_2 core/mesoporous TiO_2 shell. J Solid State Chem 178:1818–1824